Advances and Applications in Mechanical Engineering and Technology
Volume 4, 2013, Pages 1-17

THE EFFECT OF DRYING METHODS ON THE TEXTURAL PROPERTIES OF THE PSEUDOBOEHMITE SYNTHESIZED BY HOMOGENEOUS PRECIPITATION

ADRIÁN ZAMORATEGUI, JULIO A. SOTO and SATOSHI SUGITA

Department of Chemistry
University of Guanajuato
Guanajuato, Gto.
México
e-mail: azamorateguim@hotmail.com

Abstract

Pseudoboehmite was prepared by using basic aluminum sulphate as a raw material, which was synthesized by homogeneous precipitation. This BAS was neutralized in solid/liquid reaction with ammonium hydroxide in order to transform to aluminum hydroxide. The hydroxide was dried by three different routes: spray drying, freeze drying, and oven drying. The effect of the drying methods on the final textural properties of the heat treated pseudoboehmite was evaluated. Spray drying was the best route to obtain high surface area $(384 m^2/g)$ for pseudoboehmite heat treated at 450ºC (γ-Al_2O_3). It was better than the obtained by the use of freeze and oven dried routes as indicated by BET analysis (350 and 332 m^2/g), respectively. Homogeneous precipitation offers the possibility to obtain γ-Al_2O_3 powder with a high specific surface area $(ca.\ 400 m^2/g)$ and fibrous morphology.

Keywords and phrases: homogeneous precipitation, pseudoboehmite, spray drying, freeze drying, oven drying.

Received November 25, 2012; Revised December 15, 2012.

1. Introduction

All powder properties, processing procedures, and requirements vary widely between industries and applications. However, all powder processing operations share a common goal to effectively process the powder to ensure the quality and performance of the final product. This is especially important if the particle size of the powder is in the nano or micron range. The synthesis strategy of nanoparticles can be done in liquid, solid or gas phases and the methods can be divided into four main groups: synthesis of particles from the solution of the corresponding salts by controlled addition of ions; hydrolysis; thermal decomposition; or synthesis in aerosols [1-3]. Hydrolysis of inorganic salts represents a promising method for the synthesis of materials with a variety of properties and applications. It is very important to control particle size, particle size distribution, morphology, and porosity to improve the properties of pseudoboehmite powder in catalysis, composite reinforcement applications, coatings, and alumina derived ceramics [2, 5]. The homogeneous precipitation allows one to obtain spheroid particles with controlled chemistry and textural properties [6, 7]. Aluminum sulphate and ammonium bisulphite solutions have been used to synthesize spherical particles of basic aluminum sulphate (BAS). The BAS is neutralized in a solid/liquid reaction with an ammonia solution in order to transform it into aluminum hydroxide $Al(OH)_3$. Then, the hydroxide is dried to obtain the γ-AlOOH (pseudoboehmite) [8-10].

It is known that the morphology and properties of powders have been found to depend strongly on the chemical compositions and the experimental conditions used during synthesis [11-13]. The size of the pore in the obtained hydroxide can have a very wide range [14, 15]. Since the porous structure of the material is generated in the drying stage, it depends on various conditions such as the rate of heating-drying of the precipitate. Under atmospheric drying, convection is the main mode of heat transfer. The main disadvantages of this drying technique are the nonuniformity of the product, the slower drying rates compared to other drying methods, and the quality of the resulting product [16]. Spray

drying is the transformation of feed from a fluid state into a dried product by spraying the feed into a hot-drying medium. It is a one step, continuous particle-processing operation. The resulting dried product constitutes a powder, granules or agglomerates, and its form depends upon the physical and chemical characteristics of the feed and the dryer design and operation [17-19]. The objective of this paper is to analyze the effects of drying methods on the textural properties of pseudoboehmite synthesized by homogeneous precipitation.

2. Experimental Procedure

The aluminum hydroxide was obtained as described by Sugita et al. [6]. Aluminum sulphate was used as the raw material, which was dissolved in distilled water and filtered to remove insoluble materials. Thus, a clear solution was obtained. The concentration of the solution was then adjusted to 0.3M with distilled water. On the other hand, an ammonium bisulphate solution was used as precipitant, which was prepared by reacting gases between ammonia and sulphur dioxide in distilled water.

Aluminum sulphate and ammonium bisulphate solutions were mixed at a volume ratio 3:1. When the ammonium bisulphate solution is heated at 70°C, it decomposes into sulphur dioxide and ammonia. The hydrolysis of ammonium bisulphite gradually increases the pH of the solution to about 5, which is sufficient to precipitate the BAS. The precipitation was carried out for 30 minutes at 90°C. The precipitate was filtered and then washed with hot water. The solid was dispersed in water and then was treated with hot ammonia solution, to neutralize the BAS in the solid/liquid reaction. Later, the aluminum hydroxide obtained was filtered and washed with hot distilled water. This fresh aluminum hydroxide (AH) was used as a precursor for pseudoboehmite, which was dried by three routes: oven drying, spray drying, and freeze drying.

In the oven drying (OD) technique, the AH was introduced in an electric oven and heated at 120°C for 12 hours to remove the water, where it was transformed to pseudoboehmite (PBOD). In the spray drying (SD) route, the AH was dispersed in distilled water in a solid: liquid ratio of

1:40 without a dispersant. This suspension was dried in an ADL31 mini Spray Dry Tamayo at 170ºC and the pseudoboehmite powder was obtained (PBSD). Finally, for the freeze drying method (FD), the AH was frozen at – 70ºC in a Forms 86-C UTL ultra freezer from Thermo Electron Co. It was freeze dried to − 40ºC at 89×10^{-3} milibars in a LABCONCO Freeze Dry/SHELLFREEZE System, Model Freezone 6 and thus the pseudoboehmite powder was obtained (PBFD). Finally, all the pseudoboehmite powders were milled in a mortar to break down the agglomerates and heat-treated at 450, 550, 650, 750, 950, and 1250ºC for 3 hours.

The samples were examined by SEM and TEM with the microscope model JSM-6400, JEOL and a microscope model Tecnai F20 Field Emission, Philips electron microscope, respectively. A surface area and pore size analizer (ASAP 2010 Micromeretrics, USA) was used to study the N_2 adsorption-desorption isoterm at 77K.

Thermogravimetric analyses were conducted in TGA/DTA (TA Instrument: DMA, SDT 2960) in a flowing air atmosphere at a heating rate of 10ºC/min from 25 to 1300ºC by using an alpha alumina (α-Al_2O_3) as the reference material. Crystalline phase development was followed by a conventional X-ray diffraction technique using a Siemens D500 Difractometer between 10º and 80º, with monochromatic CuKα radiation, filter of Ni at 30kV.

3. Results and Discussion

3.1. Thermal behaviour of pseudoboehmites

Thermal transformation of pseudoboehmite samples was studied, and DTA curves are shown in Figure 1. Two endothermic peaks can be observed at 120ºC and 250ºC. The first endothermic with a weight loss is related to removal of physically adsorbed water, while the second endothermic weight loss corresponds to the dehydroxylation process [20].

DTA curves of PBFD, PBOD, and PBSD samples show the same thermal behaviour after 600ºC. At this temperature, all the pseudoboehmite samples had been transformed completely to γ-Al_2O_3. Thus, after the total transformation of the pseudoboehmites to γ-Al_2O_3, the three samples present the same thermal behaviour, except for the peaks corresponding to the transformation of the α-Al_2O_3 phase that are observed at different temperatures due to the drying type used to obtain the precursor material.

Thus, the DTA curve for the PBFD below 600ºC has different behaviour with respect to the PBOD and PBSD samples. As shown in Figure 2, the base line of the PBFD TGA curve lies below the PBOD and PBSD curves. This fact can be explained in the following form: This difference of temperature between the sample and the reference (α-Al_2O_3) depends on the total enthalpy required for the elimination of water. It is necessary to mention that PBFD as shown in TGA curves (Figure 2) contains a larger amount of water than the other two samples. Consequently, the difference of temperature must be bigger, that is to say, its base line should be lower than the curves corresponding to the PBOD and PBSD samples.

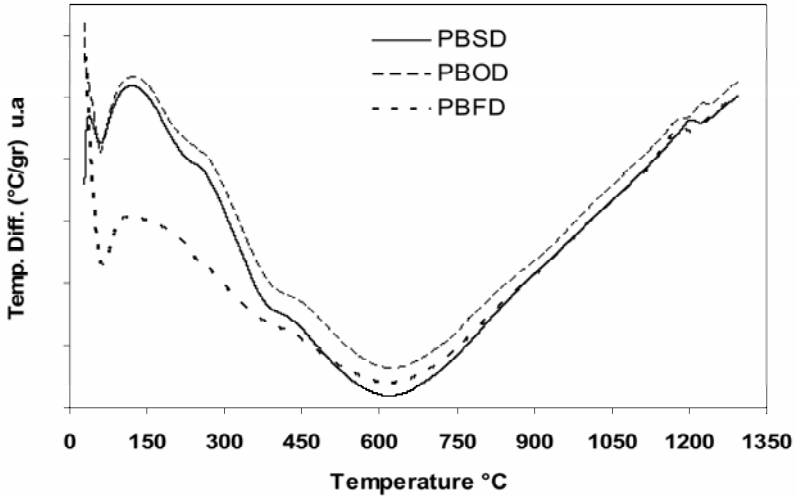

Figure 1. DTA curves for the PBFD, PBOD, and PBSD samples.

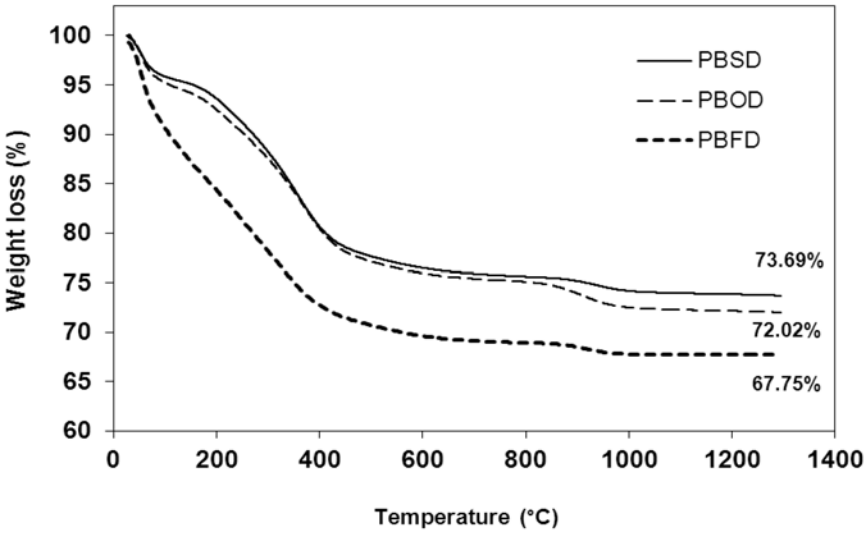

Figure 2. TGA curves of the PBFD, PBOD, and PBSD samples.

TGA curves between 28ºC and 1300ºC present weight losses at 120, 250, 400ºC and another small weight loss at about 900ºC. The percent of such weight losses are summarized in Table 1. As shown in Figure 2, the sample PBFD has the highest total weight loss (32.25wt%), in contrast with the samples PBSD and PBOD, whose weight losses are 26.31wt% and 27.98wt%, respectively. Furthermore, at 900ºC, the PBFD sample has less weight loss (1.68wt%) than the other samples (3.59wt% for PBOD and 1.92wt% for PBSD). It is necessary to mention that these percentages in weight are based on the weight of the corresponding alpha alumina.

Table 1. Weight loss of pseudoboehmites (γ-AlOOH) samples between 28 to 1300ºC

Temperature (ºC)	Weight loss (%)		
	PBSD	PBOD	PBFD
28-120	4.48	5.24	10.82
120-400	14.91	14.35	16.44
400-800	5.02	5.33	3.83
800-1000	1.42	2.59	1.14
1000-1300	0.48	0.47	0.02

It is important to notice that DTA curves of the PBFD samples show the peak of alpha phase transformation at 1195ºC. This is less than the 1220ºC and 1240ºC observed for the same transition in the PBSD and PBOD samples, respectively (Figure 3). The low temperature to transform α-Al_2O_3 can be due to the fact that more amorphous nanofibers are produced by the FD route in comparison with the SD and OD routes as was observed by X-ray diffraction. The high surface area of nanoparticles additionally supplies a substantial sintering driving force by which the sintering temperature can be slightly lowered [21].

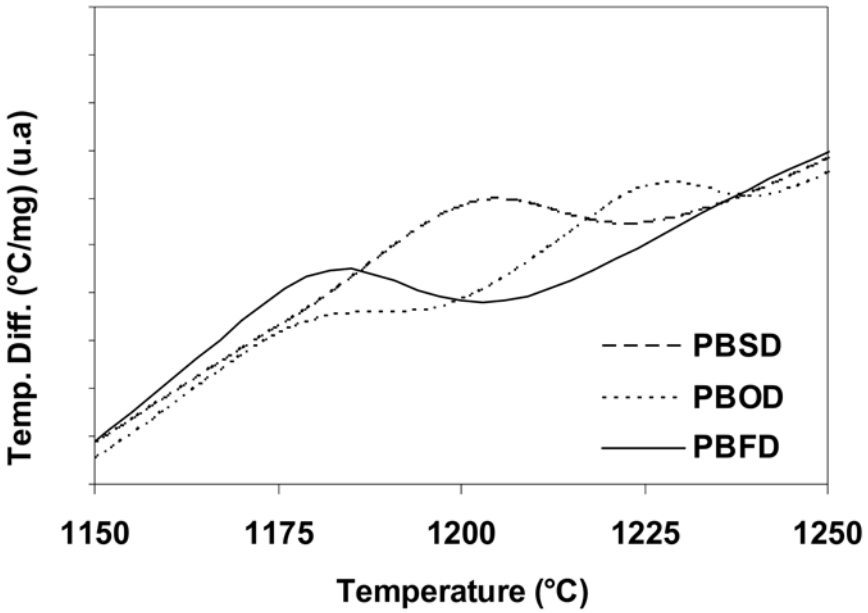

Figure 3. The effect of the drying method on the temperature of transformation to the α-Al_2O_3 phase.

3.2. XRD analysis

Crystalline structures of the BAS and PB´s were studied with XRD. Figure 4 shows the X-ray diffractograms of the original BAS precursor and pseudoboehmite synthesized by different drying routes. The BAS obtained by homogeneous precipitation is an amorphous material as shown in Figure 4(a). This BAS was neutralized in a solid/liquid reaction in order to obtain the PB by different drying method (b) PBFD; (c) PBOD; and (d) PBSD. All samples show the characteristic broad XRD peaks of pseudoboehmites at about 0.67, 0.31, 0.23, 0.18, 0.14, and 0.13 nm, as shown in the Figure 4(b)-(d) [17, 20].

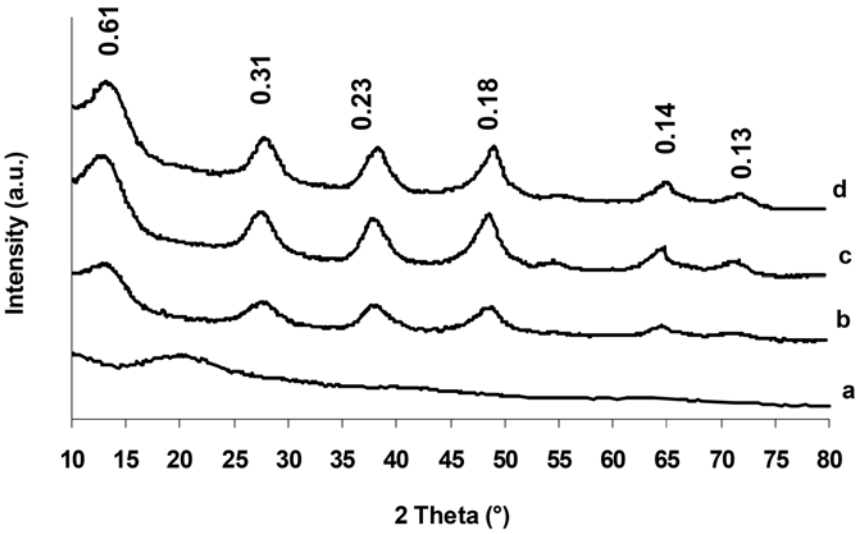

Figure 4. Powder X-ray diffraction curves of: (a) BAS; (b) PBFD; (c) PBOD; and (d) PBSD heated at 120ºC.

However, smaller peaks are observed in the corresponding diffractogram of the PBFD sample (Figure 4(b)). Also, the peak (0.14) of this sample located in the angle 2 theta corresponding to 71.5 is not easily observed and it is observed in the diffractograms of the samples PBOD and PBSD (Figure 4(c)-(d)). As would be expected, the PBOD and the PBSD reflect a higher crystallinity in agreement with DTA results shown in Figure 1. In fact, the powder obtained by freeze drying in the sample PBFD is achieved at low temperature (– 40ºC), as was described above. This kind of drying generates softer solids in contrast with the powder crystallinity obtained by the other two drying methods studied in this study. However, the OD and SD routes require increasing the temperature to 120ºC and 170ºC, respectively, to eliminate the absorbed water of the samples. The low crystallinity achieved of the PBFD sample can be attributed to the small growth of the crystals due to the water freezing at a low temperature. Thus, the PBFD powder is more amorphous because the peaks observed in Figure 4(b) are slightly smaller according to the results observed in the corresponding DTA as shown in Figure 1.

The crystalline phase evolution of the PBOD was studied at temperatures ranging from 350ºC to 1250ºC. Figure 5(b) shows that the γ-Al_2O_3 phase occurs at 450ºC, which is in agreement with thermal analysis shown in Figure 1.

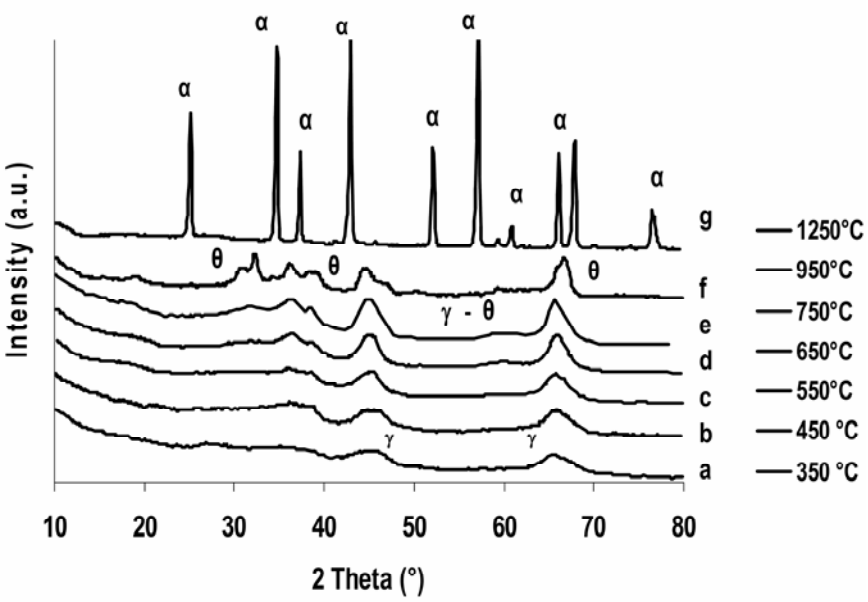

Figure 5. X-ray diffraction of PBOD sample heated at different temperatures (350ºC-1250ºC): $\gamma = \gamma$-Al_2O_3, $\theta = \theta$-Al_2O_3, and $\alpha = \alpha$-Al_2O_3.

The peaks observed in XRD patterns match well with the γ-Al_2O_3 peaks reported in the JCPDS No. 10-0425. The heat-treated γ-Al_2O_3 phase was found to persist even at a temperature of 750ºC (Figure. 5(e)). However, the theta phase (θ-Al_2O_3) starts to appear at 750ºC, which exists as the only phase at 950ºC (Figure 5(f)). At 1250ºC, the α-Al_2O_3 was identified as the only phase (Figure 5(g)).

3.3. Particle size and morphology by SEM and TEM

The scanning and transmission electron microscope was used to evaluate the effect of the drying route on the shape and particle size of pseudoboehmite. Figure 6 shows the SEM photographs of pseudoboehmites powders synthesized by OD, SD, and FD route. The powder morphology consists in spheroidal nanoparticles of around 30 nm agglomerated in all samples. The images show that the drying route does not affect the agglomerate size. On the other hand, the morphology of the pseudoboehmites observed by TEM shows that the spheroidal nanoparticles are formed by nanofibers as can be observed in Figure 7. In comparison, the PBFD sample shows much thinner and disordered nanofibers (Figure 7(b)) than that obtained by other drying routes. This can be a reason that the sample was more amorphous according to XRD analysis (Figure 4(b)).

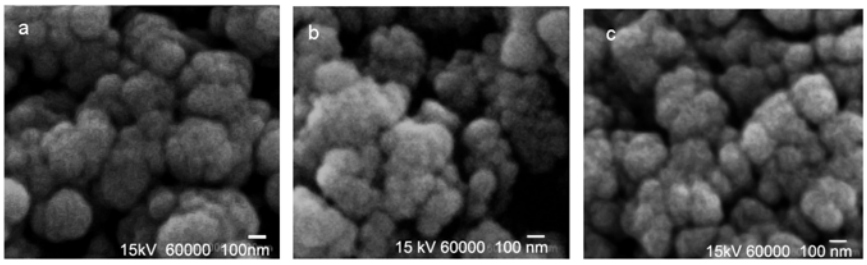

Figure 6. SEM pseudoboehmite photographs: (a) oven drying (PBOD); (b) freeze drying (PBFD); and (c) spray drying (PBSD).

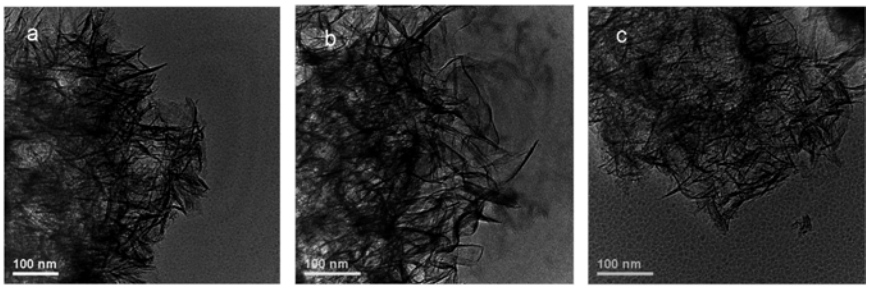

Figure 7. TEM microphotographs: (a) PBOD; (b) PBFD; and (c) PBSD.

In contrast, PBOD has thicker nanofibers than the PBFD, which seem to be slightly ordered (Figure 7(a) and (b)). In fact, the size and form of nanofibers is an effect of the drying route and FD presents a more remarkable effect than the other routes, since the sample was freeze-dried at – 70ºC and then it was freeze dried to – 40ºC limiting the growth of the crystal structure under these conditions. Since at low temperature, the crystalline structure does not grow enough, the PBFD powder shows low crystallinity (Figure 4(d)). So, the PBOD powder presents slightly thicker nanofibers probably due to the fact that the technique is developed in a static state and at a high temperature (120ºC). The sample is dried for a longer time by the OD route and the material appears to be more crystalline than PBFD according to XRD analysis (Figures 7(a) and 4(c)).

3.4. N_2 adsorption/desorption isotherms

Nitrogen adsorption and desorption were measured to investigate the effect of drying methods (SD, FD, and OD) on the textural properties of heated pseudoboehmites. Figure 8 shows the isotherms of each PB and the corresponding γ-Al_2O_3, presenting type IV isotherm (definition by IUPAC), which is characteristic for mesoporous materials. All the samples synthesized by different drying methods exhibit the same kind of isotherms with a hysteresis loop, indicating the presence of a small amount of large mesopores in the sample and the presence of “ink-bottle” type pores.

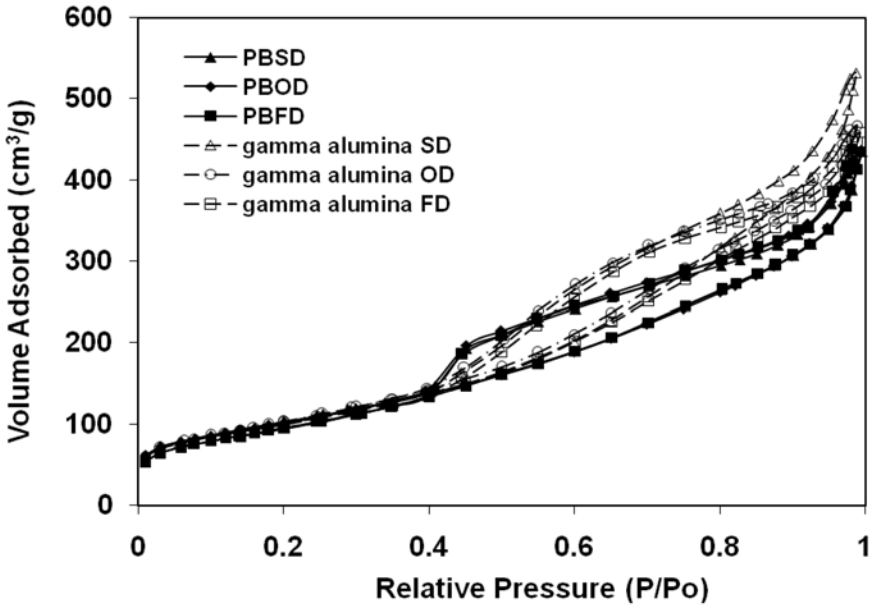

Figure 8. Nitrogen adsorption/desorption isotherms of pseudoboehmite and its corresponding gamma alumina synthesized by the three drying routes.

The pore size distribution calculated from the desorption using the BJH model is quite narrow with a maximal peak around 4.0, 4.08, and 4.64nm (Figure 9), but the average pore size is about 7.6, 8.3, and 9.0nm for the PBSD, PBFD, and PBOD, respectively, and this is due to the presence of "ink-bottle" type pores. The pore size of the corresponding γ-Al_2O_3 show more distribution due to the thermal dehydration of the PB used as a precursor. Furthermore, the voids produced by the water removed increase the specific surface area of the γ-Al_2O_3 powder. These results confirm that mesoporous pseudoboehmite can be synthesized by homogeneous precipitation and the drying route does not affect the porous morphology because all samples of PB exhibit the same pore size distribution curves. However, the specific surface area (BET) is affected by the use of different drying methods. Thus, the PBSD has a higher specific surface area than the PBFD and the PBOD powder as it is shown in Figure 10.

Thermal stability of each sample was evaluated at the temperature range of 450ºC to 1250ºC. Figure 10 shows the surface area (BET) variation with heating temperature of the pseudoboehmite samples synthesized by the three different drying methods (SD, FD, and OD). The PBSD and PBFD restrain the high surface area up $300\,m^2/g$ at 650ºC because above this temperature, the γ-Al_2O_3 is affected and starts to change to the other phase as explained before (Figure 5). In comparison, the surface area of PBOD decreased linearly with the increase of the temperature and this sample retains only $213\,m^2/g$ up to 650ºC.

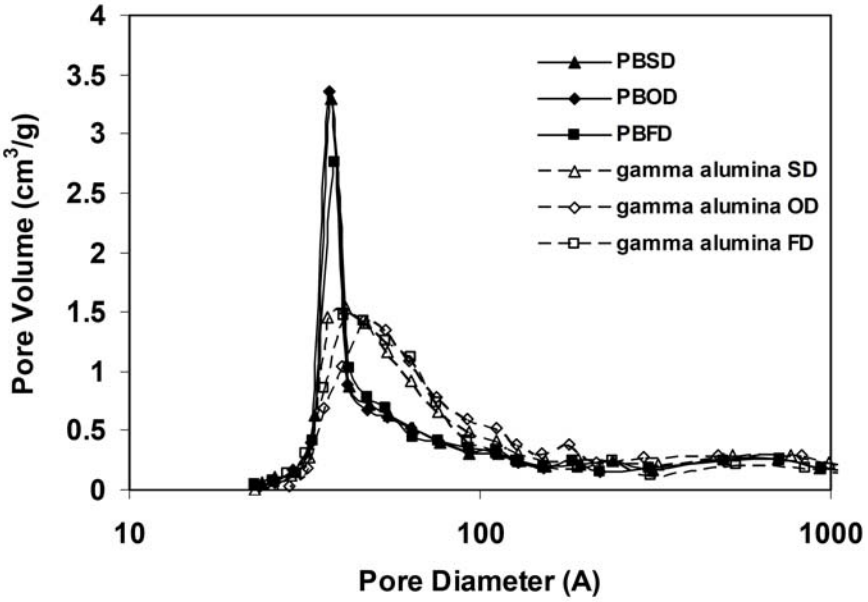

Figure 9. Pore diameter distribution of the PBSD, PBFD, and PBOD.

The homogeneous precipitation allowed for the synthesis of the γ-Al_2O_3 phase withholding specific surface areas higher than $100\,m^2/g$ and below 950ºC (where θ-Al_2O_3 phase appears). As mentioned before, the γ-Al_2O_3 phase is transformed into the θ-Al_2O_3 phase between 750ºC and 950ºC (Figures 1 and 5) and the specific surface area starts to decrease drastically (Figure 10).

Thereby, in agreement with the DTA (Figure 4), the theta phase is transformed to the alpha phase at around 1200°C. Thus, the surface area of the α-Al_2O_3 phase lies below $10 m^2/g$ as it is shown in Figure 10. The PBSD presents the best thermal stability compared with PBFD and PBOD samples because it retains more surface area than these.

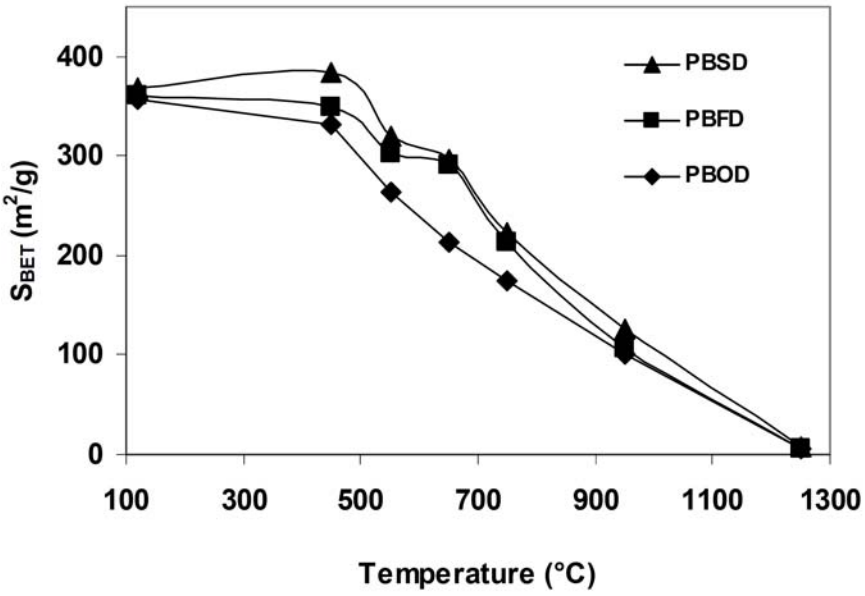

Figure 10. Variation of the specific surface areas of the pseudoboehmites with the heat treated temperature.

4. Conclusion

The aim of this study was to study the drying route effect on the textural properties of pseudoboehmite synthesized by homogeneous precipitation. This methodology followed by the solid/liquid neutralization allowed for the obtention of pseudoboehmite with spheroidal nanoparticles of about 30 nm. These spheroidal nanoparticles are formed by nanofibers of length about 75 nm and 25 nm in diameter. The size and nanofiber order is affected by the drying route. However, the size and disordered nanofibers in PBFD, do not improve the textural properties of

the gamma alumina nanopowder because of the amount of structural water. Thus, the spray drying method is better because it improves the specific surface area (BET) of PBSD $384\,m^2/g$, whereas the pseudoboehmite synthesized by FD and OD route have a smaller specific surface area about $350\,m^2/g$ and $332\,m^2/g$ heat treated at 450ºC, respectively. On the other hand, the PB samples obtained by SD and FD methods retain more surface area at 650ºC $(300\,m^2/g)$, in comparison with the OD sample, where the surface area diminished constantly with the heated temperature. But the pore volume and pore size is not affected by any drying route.

References

[1] R. Román, T. Hernández and M. González, Nano or micro grained alumina powder? A choose before sintering, Boletin de la Sociedad Espanola de Ceramica Vidrio 47(6) (2008), 311-318.

[2] S. C. Shen, Q. Chen, P. S. Chow, G. H. Tan, X. T. Zeng, Z. Wang and Reginald B. H. Tan, Steam-assisted solid wet-gel synthesis of high-quality nanorods of boehmite and alumina, J. Phys. Chem. C. 111(2) (2007), 700-707.

[3] C. Agrafiotis and A. Tsetsekou, The effect of powder characteristics on washcoat quality, Part I: Alumina washcoats, Journal of the European Ceramic Society 20(7) (2000), 815-824.

[4] Z. Ramli and R. Saleh, Preparation of ordered mesoporous alumina particles via simple precipitation method, Journal of Fundamental Sciences 4(2) (2008), 435-443.

[5] H. S. Potdar, K. W. Jun, J. W. Bae, S. M. Kim and Y. J. Lee, Synthesis of nano-sized porous γ-alumina powder via a precipitation/digestion route, Applied Catalysis A: General 321(2) (2007), 109-116.

[6] S. Sugita, C. Contreras, H. Juárez, A. Aguilera and J. Serrato, Homogeneous precipitation and phase transformation of mullite ceramic precursor, International Journal of Inorganic Materials 3(7) (2001), 625-632.

[7] V. K. La Mer and R. H. Dinegar, Theory, production and mechanism of formation of monodispersed hydrosols, J. Am. Ceram. Soc. 72(11) (1950), 4847-4854.

[8] A. C. Vieira Coelho, G. A. Rocha, P. Souza Santos, H. Souza Santos and P. K. Kiyohara, Specific surface area and structures of aluminas from fibrillar pseudoboehmite, Revista Matéria 13(2) (2008), 329-341.

[9] N. Lepot, M. K. Van Bael, H. Van den Rul, J. D'Haen, R. Peeters, D. Franco and J. Mullens, Synthesis of platelet-shaped boehmite and γ- alumina nanoparticles via an aqueous route, Ceramics International 34(8) (2008), 1971-1974.

[10] M. N. Rahaman, Ceramic Processing and Sintering, Marcel Dekker, Inc., New York, (1995), 115.

[11] R. Tettenhorst and D. A. Hofmann, Crystal chemistry of boehmite, Clays and Clay Minerals 28(5) (1980), 373-380.

[12] H. Hunuma, S. Kato, T. Ota and M. Takahashi, Homogeneous precipitation of alumina precursors via enzymatic decomposition of urea, Advanced Powder Technology 9(2) (1998), 181-190.

[13] P. Souza Santos, H. Souza Santos and S. P. Toledo, Standard transition aluminas, electron microscopy studies, Materials Research 3(4) (2000), 104-114.

[14] S. Nath and G. R. Satpathy, A systematic approach for investigation of spray drying processes, Drying Technology 16(6) (1998), 1173-1193.

[15] M. K. Naskar and M. Chatterjee, Boehmite nanoparticles by the two-reverse emulsion technique, J. Amer. Ceram. Soc. 88(12) (2005), 3322-3326.

[16] S. J. Lukasiewicz, Spray-drying ceramic powders, J. Amer. Ceram. Soc. 72(4) (1989), 617-240.

[17] A. Violante and P. M. Huang, Identification of pseudoboehmite in mixtures with phyllosilicates, Clay Minerals 29(3) (1994), 351-359.

[18] C. Tallón, M. Yates, R. Moreno and M. I. Nieto, Porosity of freeze-dried γ-Al_2O_3 powders, Ceramics International 33(5) (2007), 1165-1169.

[19] F. P. Faria, P. Souza Santos and H. Souza Santos, Spatial arrangement of fibrils in concentrated aqueous sols of fibrillar pseudoboehmite, Materials Chemistry and Physics 76(3) (2002), 267-273.

[20] E. M. Moroz, K. I. Shefer, D. A. Zyuzin, A. S. Ivanova, E. V. Kulko, V. V. Goidin and V. V. Molchanov, Local structure of pseudoboehmite, React. Kinet. Catal. Lett. 87(2) (2006), 367-375.

[21] M. Mazaheri, A. M. Zahedi and S. K. Sadrnezhaad, Two-step sintering of nanocrystalline ZnO compacts: Effect of temperature on densification and grain growth, Journal of the American Ceramics Society 91(1) (2008), 56-63.

[22] D. Y. Li, Y. S. Lin, Y. C. Li, D. L. Shieh and J. L. Lin, Synthesis of mesoporous pseudoboehmite and alumina templated with 1-hexadecyl-2,3-dimethylimidazolium chloride, Microporous and Mesoporous Materials 108(1-3) (2008), 276-282.

■